

Supplement of Atmos. Meas. Tech., 8, 4197–4213, 2015
<http://www.atmos-meas-tech.net/8/4197/2015/>
doi:10.5194/amt-8-4197-2015-supplement
© Author(s) 2015. CC Attribution 3.0 License.



Supplement of

Eddy-covariance data with low signal-to-noise ratio: time-lag determination, uncertainties and limit of detection

B. Langford et al.

Correspondence to: B. Langford (benngf@ceh.ac.uk)

The copyright of individual parts of the supplement might differ from the CC-BY 3.0 licence.

1 **Supplementary Information: Eddy covariance data with low SNR ratio: time-lag**
2 **determination, uncertainties and limit of detection.**

3
4 **1. Sensible heat, isoprene, and acetone fluxes**

5
6 1.1 Site description

7 Canopy scale flux measurements of sensible heat and volatile organic
8 compounds (VOCs) were recorded over the Bosco della Fontana nature reserve
9 situated north of Mantova in the Po valley, Italy (45° 11' 51" N, 10° 44' 31" E) as a
10 part of the ECLAIRE (Effects of Climate Change on Air Pollution and Response
11 Strategies for European Ecosystems) EC FP7 project. The nature reserve is a
12 233 ha area of broadleaf woodland dominated by four species: *Carpinus betulus*,
13 *Quercus robur*, *Quercus rubra* and *Qucerus cerris*. The measurement tower was
14 situated to the south-west of a cleared area in the centre of the forest.

15
16 1.2 Instrument setup

17 VOC fluxes and concentrations were recorded using a high sensitivity Proton
18 Transfer Reaction-Mass Spectrometer (PTR-MS, Ionicon Analytik GmbH, Austria).
19 The PTR-MS was located in an air-conditioned cabin at the base of a 42 m open
20 lattice walk-up tower. Air was sub-sampled from a PFA (O.D. ½", I.D. 9 mm) inlet line
21 which ran from just below a Gill HS sonic anemometer mounted at 32 m above
22 ground level, 5 m above the canopy top, to the cabin below. Data were logged from
23 the sonic anemometer and the PTR-MS onto a single laptop using a program written
24 in LabVIEW (National Instruments, USA).

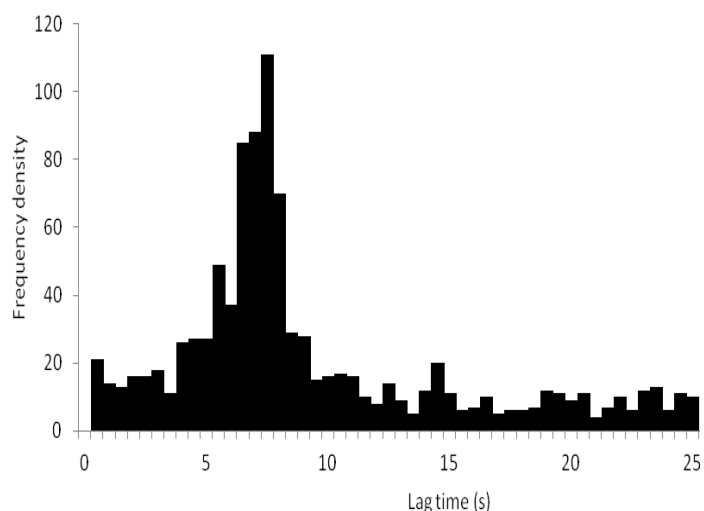
25
26 The PTR-MS operating conditions were controlled so that the reduced electric
27 field strength (the ratio of the electric field strength, E , to the buffer gas number
28 density, N) was kept to 122 Td ($1.22 \times 10^{-19} \text{ V m}^{-2}$). The drift tube temperature,
29 pressure and voltage were set to 0.21 KPa, 45 °C and 550 V respectively.
30 Measurements followed an hourly cycle with the instrument measuring zero air for 5
31 minutes followed by 25 minutes of flux measurements, 5 minutes scanning the full
32 mass spectrum and a final 25 minutes of flux measurements. While in flux mode 11
33 protonated masses were monitored at m/z 21, 33, 39, 45, 59, 61, 69, 71, 73, 81 and
34 137. These masses were assigned to the hydronium ion isotope, methanol, the
35 water cluster isotope, acetaldehyde, acetone, acetic acid, isoprene, methyl vinyl
36 ketone (MVK) and methacrolein (MARC), methyl ethyl ketone (MEK), a monoterpene
37 fragment and monoterpenes respectively. An instrumental dwell time of 0.2 s was
38 used for both m/z 21 and 39 for the other masses a dwell time of 0.5 s was applied,
39 resulting in a total measurement cycle of 4.9 seconds.

40
41 Calibration of the PTR-MS was performed using a gas standard containing
42 isoprene, acetone, and 15 other volatile organic compounds (VOCs) at a
43 concentration of approximately 1 ppmv (Ionicon Analytic GmbH, Austria).

45
46
47
48
49
50
51
52
53
54
55
56
57
58
59
60

1.3 Time-lag calculation

A constant prescribed time-lag was chosen by plotting a histogram of the empirical time-lags for isoprene, which had the largest observed fluxes and thus the cleanest cross-covariance functions. Each individual isoprene time-lag was determined by searching for the absolute maximum in the cross-covariance between isoprene mixing ratios and vertical wind velocity measurements (MAX method). Figure S1 displays a clear peak at 7.5 s which was subsequently used as the constant prescribed time-lag in this study. Many of the other measured VOCs showed weaker fluxes and hence did not display such a consistent time-lag. Consequently, the time-lags of all remaining masses were calculated by adding or subtracting the instrument dwell time from the prescribed isoprene time-lag. For example the acetic acid prescribed time-lag would be 7.0 s (7.5 s minus the 0.5 s dwell time). These measurements are presented in full by Acton et al. (2015).



61
62 **Figure S1 Histogram of the isoprene time-lags calculated by searching for the absolute**
63 **maximum in the cross-covariance function.**

64
65
66
67
68
69
70

2. Benzene fluxes

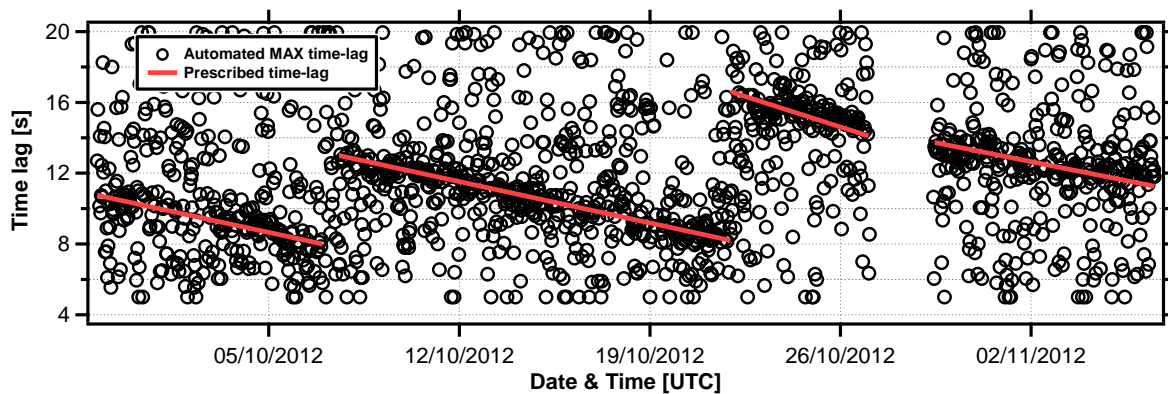
Here we present a brief description of the benzene flux measurements used in this manuscript. For a more complete detailed description please refer to Valach et al. (2015).

71 VOC flux measurements were taken from a mast on the roof of the King's College
72 Strand building (51°30'42.43"N/0° 7'0.07"W, 31 m.s.l) in Central London between 7th
73 August and 19th December 2012 as part of the ClearLo (Clean air for London)
74 project. Surrounding roads supported a medium traffic volume (annual average of
75 30k-50k vehicles per day, DfT 2014) with the river Thames situated 200 m to the

76 south. The site is classed as an urban site category 2 (intensely developed high
77 density urban with 2–5 storey, attached or very close-set buildings made of brick or
78 stone, e.g. old city core) by criteria from Oke (2006).

79 The inlet and CSAT3 sonic anemometer (Campbell Scientific) were mounted on a
80 triangular tower (Aluma T45-H) at approx. 50 m (2.2 x mean building height, z_H)
81 above ground level (Kotthaus and Grimmond, 2012). A 20 m $\frac{1}{2}$ " OD (I.D. 10 mm)
82 PFA tube inlet line was sub-sampled using the same high sensitivity proton transfer
83 reaction – mass spectrometer (PTR-MS, Ionicon Analytik GmbH, Innsbruck, Austria)
84 described above (see Lindinger et al., 1998; De Gouw and Warneke, 2007 for more
85 detailed description of the instrument), which was used to measure VOC
86 concentrations. Data from the sonic anemometer were logged at a frequency of 10
87 Hz and flux calculations were averaged over 25 minute periods. The mean line flow
88 rate was 81 l min^{-1} of which the PTR-MS sub sampled air at $0.25\text{-}0.3 \text{ l min}^{-1}$.
89 Operating parameters were controlled to maintain an E/N ratio of 122 Td. The
90 instrument was operated in MID (Multiple Ion Detection) and SCAN modes in the
91 following duty cycle: 5 min zero air (ZA), 25 min MID followed by a further 5 min
92 SCAN and 25 min MID mode. During the ZA cycle air was pumped through a
93 custom-made gas calibration unit (GCU) fitted with a platinum catalyst heated to 200
94 °C to provide instrument background values. The SCAN mode measured the
95 concentrations of a wide range of masses (m/z 21 – 206 using 0.5 s per m/z). In
96 MID mode, the quadrupole scanned 11 predetermined protonated masses with a
97 dwell time of 0.5 s for all but m/z 21 which was sampled at 0.2 s. The duty cycle
98 used comprised of the following masses: m/z 21 (indirectly quantified m/z 19 primary
99 ion count [$\text{H}_3^{18}\text{O}^+$]), m/z 33 (methanol), m/z 39 (indirectly quantified m/z 37 first
100 cluster [$\text{H}_3^{16}\text{O}^+ \text{H}_2^{16}\text{O}^+$]), m/z 42 (acetonitrile), m/z 45 (acetaldehyde) m/z 59
101 (acetone/propanal), m/z 69 (isoprene/furan), m/z 79 (benzene), m/z 93 (toluene), m/z
102 107 (C_2 -benzenes) and m/z 121 (C_3 -benzenes).

103 Measurements of turbulence and VOC concentrations were logged on separate
104 computers which meant the two dat sets had to be carefully synchronised during
105 post processing. Data synchronisation was achieved by searching for the absolute
106 maximum in a cross-covariance function between the vertical wind velocity and the
107 VOC concentrations. As well as correcting for drift between the two PC clocks, the
108 cross-covariance also accounted for the time-lag between sonic and PTR-MS
109 measurements associated with the long inlet line used. Acetone showed the clearest
110 cross-covariances which are shown in Fig. S2. A prescribed time-lag for acetone
111 was calculated based on the clustering of time-lags seen in Fig S2. Time-lags for all
112 other species were derived from this prescribed time-lag ensuring to take into
113 account the sequential nature of the PTR-MS duty cycle e.g. adding or subtracting
114 time depending on the m/z position relative to acetone in the PTR-MS duty cycle.



115

116 **Figure S2. Time series of time-lags derived for acetone fluxes by searching for the maximum in**
 117 **the cross-covariance between the vertical wind velocity and acetone concentrations. The red**
 118 **line shows the prescribed time-lag which was fit to the data.**

119 **3. N₂O fluxes**

120

121 Fluxes of N₂O were measured above two intensively managed grassland fields at
 122 the Easter Bush field site, Penicuik, Scotland in 2003. Concentrations of N₂O were
 123 measured using a tunable diode laser (TDL) absorption spectrometer (Aerodyne
 124 Research Inc., Billerica, MA, USA) at a rate of between 5 and 7 Hz. Further details of
 125 the instrument setup, site description and results can be found in Jones et al. (2011).

126

127 **4. Particle number fluxes**

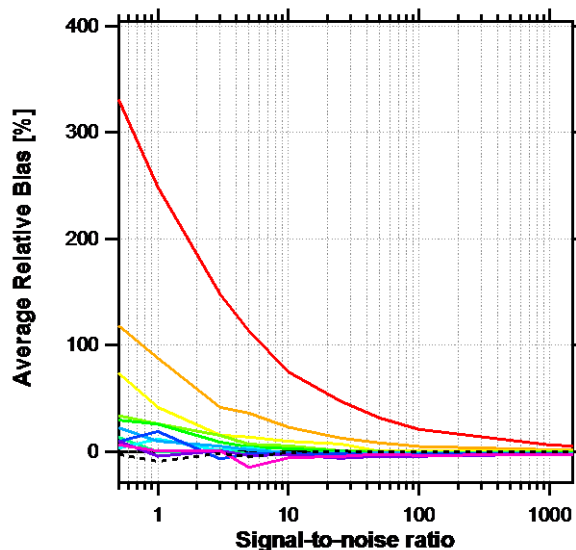
128

129 Eddy covariance particle number fluxes were made in 2009 above Speulder Bos
 130 forest (52°22'N, 05°32'W, 20 m asl), a mature Douglas fir forest located in the
 131 Netherlands. Measurements were made 8 m above the top of the 28 m tree canopy
 132 from a 45 m tall walk-up tower. Particle number concentrations were measured at 10
 133 Hz using an ultra-high sensitivity aerosol spectrometer (UHSAS, Droplet
 134 Measurement Technologies, Boulder, CO, USA) and combined with vertical wind
 135 velocity measurements from a sonic anemometer (R3, Gill Instruments, Lymington,
 136 U.K.) to give size segregated particle number fluxes (0.08 and 0.8 μm).

137

138 **5. Bias effects of different time-lag determination methods**

139 Figure S3 relates to Fig. 6 in the main manuscript and shows the average relative
 140 bias between unmodified and noisy sensible heat fluxes when calculated using a
 141 disjunct sampling interval of 5 s.



142
 143 **Figure S3.** Average relative bias of a half-hourly flux as a function of the analyser signal-to-
 144 noise ratio for 31 days of sensible heat flux data. Fluxes were calculated using the disjunct
 145 eddy covariance method with a 5 s sampling interval. The signal-to-noise ratio of the
 146 temperature data was deteriorated to match pre-defined limits. The errors shown are relative to
 147 the sensible heat flux calculated using the unmodified temperature data and a constant (0 s)
 148 time-lag.

149
 150 **References**

151
 152 Acton, W. J. F., Schallhart, S., Langford, B., Fares, S., Valach, A., Rantala, P.,
 153 Hewitt, C. N. And Nemitz, E.: Comparison of three methods to derive canopy-scale
 154 flux measurements above a mixed oak and hornbeam forest in Northern Italy, In
 155 preparation for Atmos. Chem. Phys. Discuss., 2015.
 156
 157 Davison B., Taipale R., Langford B., Misztal P., Fares S., Matteucci G., Loreto F.,
 158 Cape J.N., Rinne J. and Hewitt C.N.: Concentrations and fluxes of biogenic volatile
 159 organic compounds above a Mediterranean macchia ecosystem in western Italy.
 160 Biogeosciences, 6, 1655-1670, 2009
 161
 162 de Gouw, J. and Warneke, C.: Measurements of volatile organic compounds in the
 163 Earth's atmosphere using proton-transfer-reaction mass spectrometry, Mass
 164 Spectrometry Reviews, 26, 223-257, 2007.
 165
 166 Jones, S. K., Famulari, D., Di Marco, C. F., Nemitz, E., Skiba, U. M., Rees, R. M.,
 167 and Sutton, M. A.: Nitrous oxide emissions from managed grassland: a comparison
 168 of eddy covariance and static chamber measurements, Atmospheric Measurement
 169 Techniques, 4, 2179-2194, 2011.
 170
 171 Kotthaus, S., & Grimmond, C. S. B.: Identification of Micro-scale Anthropogenic CO₂,
 172 heat and moisture sources – Processing eddy covariance fluxes for a dense urban
 173 environment. Atmospheric Environment, 57, 301–316.
 doi:10.1016/j.atmosenv.2012.04.024, 2012.

174 Lindinger, W., Hansel, A., and Jordan, A.: On-line monitoring of volatile organic
175 compounds at pptv levels by means of proton-transfer-reaction mass spectrometry
176 (PTR-MS) - Medical applications, food control and environmental research, Int. J.
177 Mass Spectrom., 173, 191-241, 1998.
178
179 Oke, T. R.: Towards better scientific communication in urban climate, Theoretical
180 and Applied Climatology, 84, 179-190, 2006.

181 Taipale R., Ruuskanen T.M., Rinne J., Kajos M.K., Hakola H., Pohja T., and Kulmala
182 M.: Technical Note: Quantitative long-term measurements of VOC concentrations by
183 PTR-MS – measurement, calibration, and volume mixing ratio calculation methods.
184 Atmospheric Chemistry and Physics, 8, 6681-6698, 2008
185
186 Valach A., Langford B., Nemitz E., MacKenzie A. R., and C. N., Hewitt.: Seasonal
187 trends in volatile organic compound fluxes and concentrations above central London.
188 Atmospheric Chemistry and Physics Discussions. In preparation (2015).
189
190
191